Liquefaction-induced Downdrag on Piles and Drilled Shafts

V. Noel Vijayaruban[1], B. Muhunthan[2], B. H. Fellenius[3]

ABSTRACT

Liquefaction-induced downdrag varying from near zero to excessive in drilled shafts and pile foundations were observed in the February 7, 2010 Maule Magnitude 8.8 earthquake in Chile. This study presents an analytical method to account for liquefaction-induced downdrag in piles and drilled shafts. The method is based on the neutral plane concept extended to handle multiple liquefiable zones. The proposed method is illustrated on a field case history from the Chile earthquake. Four representative locations were considered along the bridge, where analysis of boreholes identified the potential for multiple liquefiable zones within and below the pier embedment depth. The drag force, downdrag, and neutral plane depth were computed. Axial load distributions for short-term and long-term were computed using the available SPT N-indices. The maximum possible toe penetration was estimated for one of the extreme conditions. It was noticed that the liquefaction-induced downdrag was small as opposed to the observed settlements.

Introduction

Sandy soil layers reduce volume during and following liquefaction (Tokimatsu and Seed 1987, Ishihara and Yoshimine 1992). The volume reduction appears as a downward movement—settlement—of the overlying soil layers. For piled foundations, such movement may influence the load distribution on the pile. Depending on the site conditions, the change in axial response resulting from liquefaction-induced downdrag can have a significant impact on the pile performance as demonstrated in the February 7, 2010, Magnitude 8.8, earthquake in Chile, where liquefaction-induced settlement on piers and piles ranged from near zero to excessive (Yen et al. 2011).

Methods to account for liquefaction effects on piled foundations are addressed in terms of drag force development in a few design manuals, such as AASHTO (2007). Development of drag force in piles and drilled shafts constructed in consolidating soils have been addressed by several authors, (e.g., Fellenius 1984; 2004, Poulos and Davis 1990). Only a few analytical studies have addressed drag force and downdrag where the soil settlement is caused by seismic liquefaction, (e.g., Boulanger and Brandenberg 2004, Rollins and Strand 2006, Fellenius and Siegel 2008). Fellenius and Siegel (2008) applied the Unified Method (Fellenius 1984; 2004; 2014) to the effect of seismic liquefaction—a method based on interaction between pile resistance and soil settlement. The method involves re-positioning the neutral plane following a liquefaction event considering the liquefied zone relative to the neutral plane. Several potentially liquefiable zones within pier embedded length and below pier toe were observed in the case of 2010 Chile earthquake, which presents the need to extend the recommendations by Fellenius and Siegel (2008) to include multiple liquefiable zones as is addressed in the present study.

Reconnaissance teams from the Earthquake Engineering Research Institute (EERI) and the

[1]Geotechnical Engineer, CH2M, Santa Ana, CA, USA, Noel.Vijayaruban@ch2m.com
[2]Professor & Chair, Dept. of Civil & Envir. Eng., Washington State University, WA, USA, muhuntha@wsu.edu
[3]Consulting Engineer, Sidney, BC, Canada, bengt@fellenius.net

Geotechnical Extreme Events Reconnaissance (GEER) documented liquefaction-induced downdrag incidences and associated failures of a number of bridge piers across the Bío-Bío River in Concepcion, Chile. The Juan Pablo II Bridge is the best documented of these cases.

The Maule Chile Earthquake and the Juan Pablo II Bridge

On February 7, 2010, a magnitude 8.8 earthquake struck in the Pacific Ocean just outside Chile. The earthquake was characterized by its long duration (>2 minutes) and strong ground motion. Recorded peak ground acceleration at Station Colegio San Pedro, Concepción was 0.65g. Many of these bridges were constructed after the mid-1950s in accordance with the AASHTO *Standard Specifications for Highway Bridge Design* (Yen et al. 2011).

The Juan Pablo II Bridge traverses the Bío-Bío River in the NE-SW direction as shown in Figure 1. It was opened to public in 1974. It is nearly 2.3 km long with more than 70 spans of 22 m wide, 33 m long concrete decks, each span having 7 reinforced concrete girders. The span supports are reinforced concrete bents founded on two 2.5 m diameter and approximately 16 m long piers (Ledezma et al. 2012). The average load per pier is 12,700 kN, as estimated from the main components—concrete deck (2,150 kN), steel girders (9,600 kN), wearing surface coarse (590 kN), and bridge bent (360 kN). The piers along this bridge settled appreciably at various locations and the bridge had to be closed for public access.

Field Observations

Noticeable pier settlement and lateral displacement of the bridge decks with column shear failure and significant displacements and rotations of the bridge bents were recorded by the reconnaissance team (Yen et al. 2011). The piers settled as much as the ground surface, which indicates that the N.P. lies at the ground surface. Several sand boils were observed near the embankment as well as around the piers (Bray and Frost 2010). The volume loss from the ejecta will have contributed to reduction in the liquefied layer thickness and added to the soil settlements due to seismic compaction.

Figure 1: Pier locations and nearby boreholes at Juan Pablo II Bridge.

A total of 16 SPT boreholes were advanced to depth of 40 m outside the footprint of the bridge for the post-quake site investigation. The borehole information showed that the soil profile consists of sand, sandy silt, silty clay, and silty sand. The groundwater table was at the ground level. The report by the GEER (2010) documented that the northeast approach of the bridge suffered more than the southwest approach. For the present study, two Piers, Nos. 1-2 (BH-16) and 5-6 (BH-10), toward the southwest end of the bridge and two Piers, Nos. 117-118 (BH-3) and 119-120 (BH-7), toward the northeast were selected. Verdugo and Peters (2010) have reported a range of pier settlements along Juan Pablo II Bridge. The observed

settlements of Piers 1-2, 5-6, 117-118 and 119-120 were about 200, 400, 450, and 650 mm, respectively. A plan view of the pier locations and closest boreholes is shown in Figure 1.
Figure 2 presents N-index distributions from four boreholes (BH-3, BH-7, BH-10, and BH-16). The figures delineate the potentially liquefiable zones as determined using the Youd et al. (2001). The shaded bands represent the liquefiable zones. Three potentially liquefiable zones exist within the pier embedded lengths. The first 3 m thick zone is at the ground surface. The second and third zones are 1 and 4 m thick and located between the depths of 7 through 8 m and 9 through 13 m, respectively. In BH-3, an about 1 m thick liquefiable zone is identified right at the pile toe depth. Three additional, about 2 to 4 m thick zones exist below the pile toe starting at depths of about 25, 30, and 33 m. Variations of thickness and location of the liquefiable zones likely exist between the boreholes.
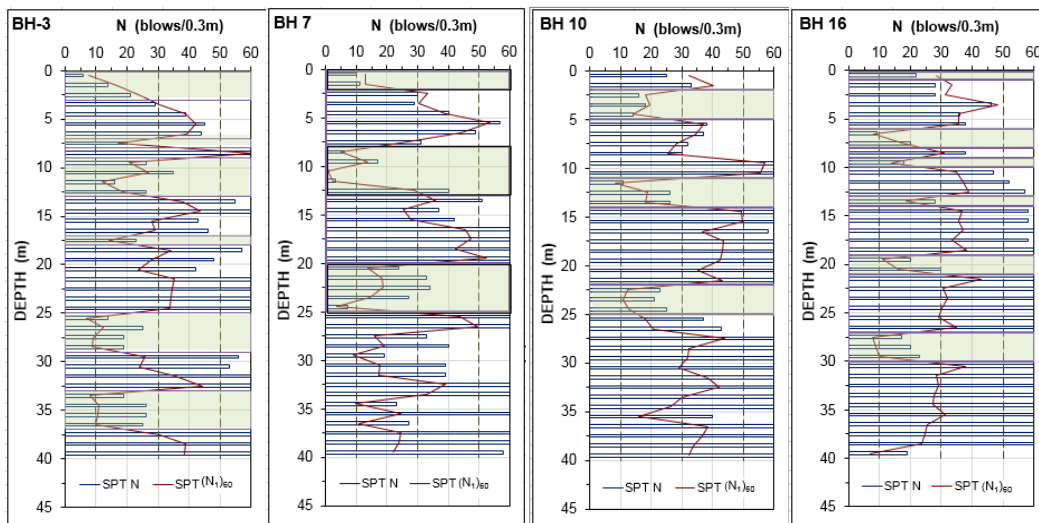

Figure 2: SPT N and $(N_1)_{60}$ values with depth and potentially liquefiable zones.

SPT N-index correction factors, such as corrections for borehole diameter (C_B), sampler type (C_S), rod length (C_R), and hammer energy ratio (C_E) are assumed to be 1.05, 1.0, 0.85, and 0.85, respectively; and maximum overburden correction factor (C_N) is 1.7. Fines content variation with depth and normalized SPT N-indices, $(N_1)_{60}$, were applied to determine the liquefiable zone identified in the figures. Additional liquefaction susceptibility key parameters, such as cyclic stress ratio (CSR), ratio of total stress to effective stress (σ_v/σ_v'), and stress reduction coefficient (r_d) are in the following ranges 0.4 - 0.9, 2.0 – 2.2, and 0.4 – 1.0, respectively. Values of $(N_1)_{60}$ below 30 blows/0.3 m were considered representative for a liquefiable zone. Although the method supposedly only applies to depths above 25 m, it has been used to delineate the liquefiable zones also below 25 m depth.
BH-7 includes two liquefiable zones, 2 and 5 m thick, at the ground level and at depths 8 through 13 m respectively. Three additional zones with varying thicknesses from 4 to 5 m are identified at depths of 20, 27, and 34 m. BH-10 also comprises two liquefiable zones between the depths of 2 through 5 m and 11 m through 14 m. Other two zones are found at depths of 22 and 34 m with thicknesses of 5 and 2 m. BH-16 consists of 4 liquefiable zones within the pier length; those thicknesses range from 1 to 2 m between depths of ground level through 1 through 8 m, 9 through 10 m, and 13 through 14 m. Four more zones were identified at depths of 19, 25, 27, and 36 m with thicknesses of 2, 1, 3, and 4 m, respectively.

Soil Settlement

Tokimatsu and Seed (1987) method was adopted to estimate the post-liquefaction volumetric compressions of liquefiable zones. The post-liquefaction settlement was calculated by integrating volumetric strain over the thickness of each liquefiable zone. Each liquefiable zone was divided into sub-zones with constant SPT N-index. The cumulative post-liquefaction settlement was obtained by adding the settlement of the individual zones. Figure 3 shows the distribution of post-liquefaction settlement calculated at the four borehole locations. It is interesting to note that about half of the soil settlement, about 150 mm through 300 mm, is estimated to have occurred below the pier toe level at all four piers.
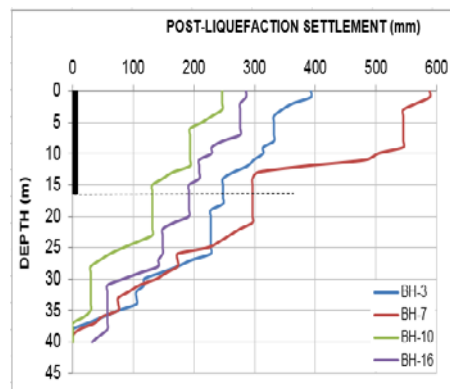

Figure 3: Post-liquefaction soil settlement profiles for BHs 3, 7, 10, and 16.

The Unified Analysis Method (Fellenius and Siegel 2008)

The Unified method is used to analysis the response of piles to load and soil movements. The principle of the load distribution curve is common for all conditions—before, during, and after liquefaction. The neutral plane (N.P.) is the intersection of the load and resistance curves. The toe resistance is governed by the toe penetration. The interdependence between the toe resistance and toe penetration determines N.P. position. Liquefaction of a zone will result in (1) loss of effective stress resulting in a corresponding loss of shaft resistance and (2) loss of volume i.e., the zone will reduce in thickness. The loss of shaft resistance will be negligible if the liquefied zone height is not significant. The reduction of soil volume may have a significant effect on the pile. If the liquefiable zone is located above the N.P., as shown in the left side of Figure 4, the load curve will translate downward, but the associated small unloading of the pile toe will show a similar upward translation of the resistance curve with the combined effect that the location of the N.P. will not change appreciably and no downdrag change will occur. The changes to axial response are unimportant for the pile. i.e., the ground will settle, but the pile will not.

When the liquefiable zone is located below the N.P., as shown in the right side of Figure 4, the loss of volume in the liquefiable zone will increase the settlement at the N.P. and, therefore, in the absence of supporting toe resistance, result in increased downdrag (settlement) for the pile(s) by the amount of the reduction in height of the liquefied zone. As shown, if there is toe bearing, the increase of toe penetration will increase the toe resistance, which will lower the N.P. and offset some of the liquefaction settlement for the pile—the pile will settle, but ground surface will then settle more than the pile.
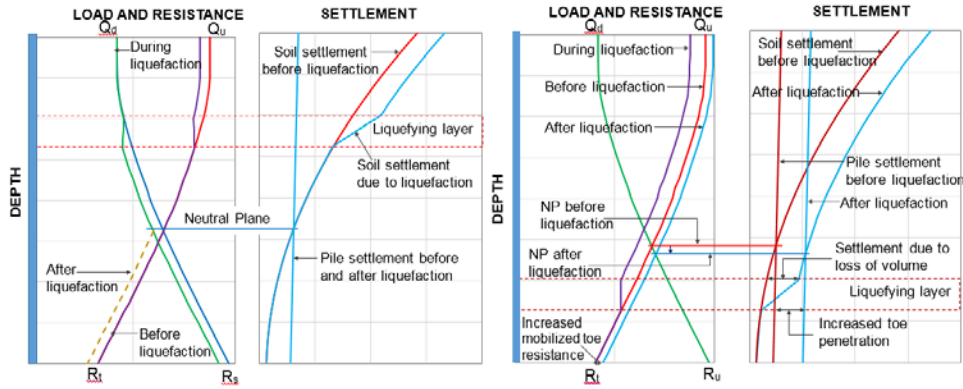
Figure 4: Typical response when the liquefying layer is located above and below the N.P.

When the liquefiable zone is located below the pile toe, no change occurs with regard to the shaft and toe resistances and location of the N.P. relative to the pile. However, the loss of volume in the liquefied zone will result in a corresponding settlement of the soil around the pile and, therefore, also of the pile and piled foundation. That is, the ground surface and the pile will settle together—by equal amounts.

As mentioned, multiple liquefiable zones within the pier embedment depth exists both above and below the N.P. at the Juan Pablo site. To account the multiple zones, Fellenius and Siegel (2008) principles of analysis can be superimposed as summarized below.

Estimation of Shaft and Toe Resistances

An effective stress analysis (beta-method) is applied to estimate the shaft and toe resistances to determine the liquefaction effect. SPT N-indices were applied to our analysis by employing the approaches suggested by Meyerhof (1976), Decourt (1982), and O'Neill and Reese (1999) for determining the effective stress beta-coefficient distribution. Meyerhof (1976) recommended that the unit shaft resistance be determined as a function of the N-index according to:

$$r_s = nN \tag{1}$$

where r_s, n, and N are unit shaft resistance (kPa), a coefficient (=1 for bored piles), and N-index (blows/0.3 m) not energy-corrected, respectively.

Decourt (1982) proposed a relation for unit shaft resistance using N-index as in Equation 2.

$$r_s = \alpha(2.8N_{60} + 10) \tag{2}$$

where r_s, α, N_{60} are unit shaft resistance (kPa), a coefficient (= 0.5 for piles in silty sand), and normalized N-index (blows/0.3 m) energy-corrected, respectively.

O'Neill and Reese (1999) suggested calculating the beta-coefficient for drilled shafts in cohesionless soil, as given in Equations 3a and 3b. The r_s is limited to 200 kPa. Note that for $(N_1)_{60} \geq 15$, the O'Neill and Reese beta-coefficient only depends on the depth, z.

$$\beta = \frac{N_{60}}{15}(1.5 - 0.245\sqrt{z}) \qquad \text{for } (N_1)_{60} < 15 \tag{3a}$$
$$\beta = 1.5 - 0.245\sqrt{z} \qquad \text{for } (N_1)_{60} \geq 15 \tag{3b}$$

where β is the beta-coefficient, z is the SPT sampling depth, $(N_1)_{60}$ is N-index (blows/0.3 m)

energy-corrected. An averaged distributions of β's were estimated by applying the three methods to the four boreholes.

The three quoted methods also include relations for pile toe resistance, considered to be ultimate values, ostensibly correlated and defined as "ultimate" by using results of static loading tests, usually by limiting the unit toe resistance to 3 MPa. However, for the subject case, no test was made and, therefore, no ultimate value is defined. Therefore, the toe relations do not apply. Instead, the pile toe response to load and pile toe penetration is assumed to follow a load-movement relation expressed in a q-z function, such as the Ratio Function expressed in Equation 4 (Fellenius 2014).

$$\frac{R_1}{R_2} = \left(\frac{\delta_1}{\delta_2}\right)^{\theta} \tag{4}$$

where R_1 and R_2 are specific toe resistances, δ_1 and δ_2 are movements mobilized at R_1 and R_2, respectively, θ is exponent usually ranging from a small value through unity, Typical θ - values for piles in sand range between 0.4 and 0.8

Load Distribution in the Piers before the Earthquake

For a short-term condition, soon after construction, the sustained load, 12,700 kN (Q_d), would have been supported by a shaft resistance R_s, and the balance being the mobilized toe resistance, R_t. Considering the averaged distribution of beta-coefficients, the load distribution would be controlled by a total shaft resistance of R_s is 5,900 kN and, the balance, therefore, is a toe resistance, R_t, equal to 6,800 kN (unit toe resistance, r_t = 1.4 MPa). The calculations consider groundwater at the ground surface, and a soil density of 2,000 kg/m^3 using the UniPile software (Goudreault and Fellenius 2013). Load distribution is shown in Figure 4.

For a long-term (1974-2010) before the earthquake, the soil around the piers will have settled at least a few millimeter, which will have resulted in negative skin friction along an upper portion of the pier, maintained the positive shaft resistance along the lower portion, and increased the toe resistance. The figure shows a probable long-term distribution for a N.P. located at a depth of about 10 m. This location corresponds to a 12,500 kN toe resistance (r_t = 2.5 MPa). When the entire pier is subjected to negative skin friction (N.P. right at the toe), the maximum toe resistance would be equal to 18,600 kN (r_t = 3.7 MPa).

Toe penetrations were calculated according to Equation 4 with an exponent, θ, of 0.5 and matched to a 10 mm pile toe movement, as assumed probable for the long-term condition. It is included in Figure 4. The toe load-movement curve indicates that the short-term, probable long-term, and maximum long-term pile toe movements are 3, 10, and 22 mm, respectively. As long as the liquefiable zone would have been located above the toe, then, the distribution labeled "maximum long-term" would also have been the maximum case for the pier after the quake. Moreover, if the sand below the toe—below 16 m depth—would have been unaffected by the quake, then, the indicated 22 mm toe movement is the maximum possible movement of the toe and, therefore, of the pier. No amount of liquefaction-induced soil settlement above the toe including the soil loss from sand boils—could then have induced any larger settlement of the piers than that shown in the figure for the maximum long-term.
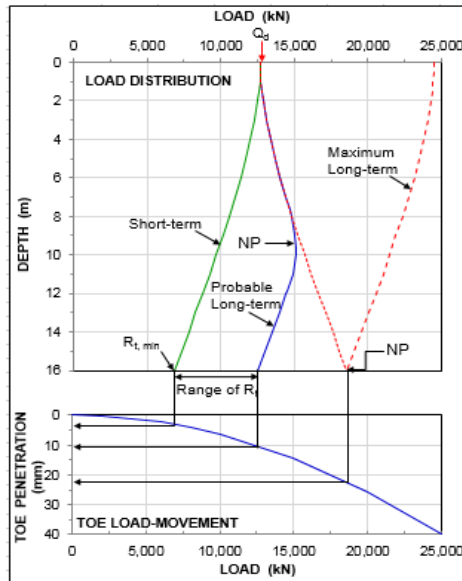
Figure 4: Load distribution for short-term and long-term conditions and corresponding toe penetration.

Since the pier settlements are much larger than 22 mm, clearly, the liquefaction affecting the piers must have occurred below the pier toe level. This is further supported by the observation (Bray and Frost 2010) that the settlement of the ground surface and that of the pier were essentially equal at several piers, which indicates that most of the settlement occurred below the pile toe. The two possible scenarios are: (1) there was a liquefiable zone at or within a distance of one or two pile diameters (2.5 through 5.0 m) below the pier toe and the liquefaction of that zone reduced the toe resistance so that the shaft resistance was insufficient to support the pier load; such piers plunge until sufficient toe resistance was gained, and (2) the pier settlement is the accumulation of volume loss in the various liquefiable zones at and below about 16 m depth. The latter would have at the most resulted in about 300 mm total settlement. As the observed settlement is much larger, we believe that a large portion of the catastrophic pier settlement is due to loss of toe resistance in liquefiable zones at or below the pier toe level.

Conclusions

Liquefaction-induced downdrag analysis was done on four representative boreholes from Juan Pablo II Bridge site. Multiple liquefiable zones were identified within the pier length and below the pier toe level. Three distinct stages—short-term, probable long-term, and maximum long-term were considered. The analysis showed very low toe movement (≈22 mm) at its maximum long-term condition. Liquefaction-induced downdrag from liquefiable zones within the pier length is limited for relatively short pile foundations. This estimated toe movement was just a fraction of the total post-liquefaction settlement. Even though the estimated pier settlements (Piers, Nos. 117-118 and 119-120) were large toward northeast approach of the bridge due to high post-liquefaction settlement, estimated pier settlements are low compared to reported values. We believe the difference in settlements might have resulted from plunging of piers due to combination effect of strong ground shaking and loss of toe resistance. This scenario brings additional settlement to the estimated values. A plunging continues until enough resistance developed to carry the load and the downdrag development come to an end. The analysis also indicates that significant post-liquefaction

settlement occurred in the soil layers well below the pile toe level.

Acknowledgements

<div align="center">

References

</div>

AASHTO (2007). LRFD Bridge Design Specifications. American Association of State Highway and Transportation Officials, 4th Ed., Washington, D.C., USA.

Boulanger, R.W., and Brandenberg, S.J. (2004). Neutral Plane Solution for Liquefaction-induced Down-drag on Vertical Pile. Proc., of Geo-Trans 2004, ASCE, Los Angeles, CA, 470-478.

Bray, J.D., and Frost, J.D., Eds., (2010). Geo-Engineering Reconnaissance of the 2010 Maule, Chile Earthquake, A report of the NSF-Sponsored GEER Association Team, primary authors: Arduino et al.

Decourt, L. (1982). Prediction of Bearing Capacity of Piles Based Exclusively on N-values of the SPT. Proc. ESOPT II, Amsterdam, pp. 19-34.

Fellenius, B.H. (1984). Negative Skin Friction and Settlement of Piles. Proc. of the 2nd Intl Seminar, Pile Foundations, Nanyang Technological Institute, Singapore, 18 p.

Fellenius, B.H. (1988). Unified Design of Piles and Pile Groups. Transportation Research Board, Washington, TRB Record 1169, pp. 75-82.

Fellenius, B.H. (2004). Unified Design of Piled Foundations with Emphasis on Settlement Analysis. Honoring George G. Goble—Current Practice and Future Trends in Deep Foundations, Geo-Inst. Geo TRANS Conf., Los Angeles, Jul. 27-30, 2004, Ed. by J.A. DiMaggio and M.H. Hussein. ASCE GSP 125, 253-275.

Fellenius, B.H. (2014). Basics of Foundation Design, Electronic Ed., <www. Fellenius.net>, 410 p.

Fellenius, B.H. and Siegel, T.C. (2008). Pile Design Consideration in a Liquefaction Event. ASCE J. of Geotech. and Environ. Engng, 132(9), 1412-1416.

Goudreault, P.A. and Fellenius, B.H. (2013). UniPile Version 5, Users and Examples Manual. UniSoft Geotechnical Solutions Ltd. [www.UniSoftGS.com], 99 p.

Ishihara, K., and Yoshimine, M. (1992). Evaluation of Settlements in Sand Deposits Following Liquefaction During Earthquakes. J. Soil Mech., Found. Engng, 118(32), 173-188.

Ledezma, C., Hutchinson, T., Ashford, S.A., Moss, R., Ardunio, P., Bray, J.D., Olson, S., Hashash, Y.M.A., Verdugo, R., Frost, D., Kayen, R., and Rollins, K.M. (2012). Effects of Ground Failure on Bridges, Roads, and Railroads. Earthquake Spectra, 28(S1), S119-S143.

Meyerhof, G.G., (1976). Bearing Capacity and Settlement of Pile Foundations. The Eleventh Terzaghi Lecture, Nov. 5, 1975. ASCE J. of Geotech. Engng 102(GT3) 195-228.

O'Neill, M.W. and Reese, L.C., (1999). Drilled Shafts. Construction Procedures and Design Methods, Federal Highway Administration, Transportation Research Board, Washington, FHWA-IF99-025

Poulos, H., and Davis, E.H. (1990). Pile Foundation Analysis and Design, Reprint Ed., Robert E. Krieger Publishing Company, Florida.

Rollins, K.M. and Strand, S.R. 2006. Downdrag Forces due to Liquefaction Surrounding a Pile. Proc. of the 8th U.S. National Conf. on Earthquake Engineering. San Francisco, Apr.18-22, Paper No. 1646, 10 p.

Tokimatsu, K., and Seed, H.B. (1987). Evaluation of Settlements in Sands Due to Earthquake Shaking. J. Geotech. Engineering, 113(8), 861-879.

Verdugo, R., and Peters, G. (2010). "Informe Geotécnico Fase Anteproyecto Infraestructura Puente." Mecano Eje Chacabuco, Rev7, Aug.2010.

Yen, W.P., Chen, G., Buckle, I., Allen, T., Alzamora, D., Ger, J., and Arias, J.G. (2011). Post-Earthquake Reconnaissance Report on Transportation Infrastructure: Impact of the February 7, 2010, Offshore Maule Earthquake in Chile." Federal Highway Administration FWWA-HRT-11-030, p.214.

Youd, T.L., Idriss, I.M., Andrus, R.D., Arango, I., Castro, G., Christian, J.T., Dobry, R., Finn, W.D.L., Harder, L.F. Jr., Hynes, M.E., Ishihara, K., Koester, J.P., Liao, S.S.C., Marcuson, W.F.III, Martin, G.R., Mitchell, J.K., Moriwaki, Y., Power, M.S., Robertson, P.K., Seed, R.B., Stokoe, K.H. II. (2001). Liquefaction Resistance of Soils: Summary Report from the 1996 NCEER and 1998 NCEER/NSF Workshop on Evaluation of Liquefaction Resistance of Soils. J. Geotech. Geoenv. Engng., 127(10), 817-833.